

UCLA

UCLA Previously Published Works

Title

GrB-Fc-KS49, an anti-EMP2 granzyme B fusion protein therapeutic alters immune cell infiltration and suppresses breast cancer growth.

Permalink

<https://escholarship.org/uc/item/7fv9x6j4>

Journal

Journal for ImmunoTherapy of Cancer, 12(12)

Authors

Mohamedali, Khalid
Aguirre, Brian
Lu, Cheng-Hsiang
et al.

Publication Date






2024-12-22

DOI

10.1136/jitc-2024-008891

Peer reviewed

GrB-Fc-KS49, an anti-EMP2 granzyme B fusion protein therapeutic alters immune cell infiltration and suppresses breast cancer growth

Khalid A Mohamedali ¹, Brian Aguirre,² Cheng-Hsiang Lu,³ Anubhav Chandla ², Nidhi Kejriwal,² Lucia Liu,² Ann M Chan,² Lawrence H Cheung,¹ SuYin Kok,² Sergio Duarte,⁴ Ana Alvarez de Cienfuegos ¹, David Casero ³, Michael G Rosenblum,¹ Madhuri Wadehra ^{2,5}

To cite: Mohamedali KA, Aguirre B, Lu C-H, *et al.* GrB-Fc-KS49, an anti-EMP2 granzyme B fusion protein therapeutic alters immune cell infiltration and suppresses breast cancer growth. *Journal for ImmunoTherapy of Cancer* 2024;**12**:e008891. doi:10.1136/jitc-2024-008891

► Additional supplemental material is published online only. To view, please visit the journal online (<https://doi.org/10.1136/jitc-2024-008891>).

Accepted 25 November 2024



© Author(s) (or their employer(s)) 2024. Re-use permitted under CC BY-NC. No commercial re-use. See rights and permissions. Published by BMJ Group.

For numbered affiliations see end of article.

Correspondence to

Dr Madhuri Wadehra;
mwadehra@mednet.ucla.edu

ABSTRACT

Background Granzyme B (GrB) is a key effector molecule, delivered by cytotoxic T lymphocytes and natural killer cells during immune surveillance to induce cell death. Fusion proteins and immunoconjugates represent an innovative therapeutic approach to specifically deliver a deadly payload to target cells. Epithelial membrane protein-2 (EMP2) is highly expressed in invasive breast cancer (BC), including triple-negative BC (TNBC), and represents an attractive therapeutic target.

Methods We designed a novel fusion protein (GrB-Fc-KS49) composed of an active GrB fused to an anti-EMP2 single-chain antibody tethered through the immunoglobulin G heavy chain (Fc) domain. We assessed the construct's GrB enzymatic activity, anti-EMP2 binding affinity, and cytotoxicity against a panel of BC cells. The construct's pharmacokinetics (PK), toxicity profile, and in vivo efficacy were also evaluated.

Results GrB-Fc-KS49 exhibited comparable GrB enzymatic activity to commercial GrB, as well as high affinity to an EMP2 peptide, with the dissociation constant in the picomolar range. The fusion protein rapidly internalized into EMP2+ cancer cells and showed in vitro cytotoxicity to cell lines expressing surface EMP2, with half-maximal cytotoxicity (IC₅₀) values below 100 nM for most positive lines. Ex vivo stability at 37°C indicated a half-life exceeding 96 hours while in vivo PK indicated a biexponential plasma clearance, with a moderate initial clearance (t_{1/2α}=18.4 hours) and a much slower terminal clearance rate (t_{1/2β}=73.1 hours). No toxicity was measured in a Chem16 panel between the control and the GrB-Fc-KS49. In vivo, the GrB-Fc-KS49 showed efficacy against a TNBC syngeneic (4T1/_{FLUC}) mouse model, reducing tumor volume and cell proliferation and increasing cell death compared with controls. Treatment using an EMT6 mouse model confirmed these results. In addition to a significant impact on cell proliferation, GrB-Fc-KS49 treatment also resulted in a dramatic increase of tumor-infiltrating CD45+ cells and redistribution of tumor-associated macrophages. Transcriptomic analysis of tumors post-treatment confirmed the remodeling of the immune tumor microenvironment by the GrB-Fc-KS49 immunotoxin.

WHAT IS ALREADY KNOWN ON THIS TOPIC

⇒ High expression of epithelial membrane protein-2 (EMP2) is observed in greater than 75% of patients with breast cancers, including those with triple-negative breast disease (TNBC).

WHAT THIS STUDY ADDS

⇒ Our results demonstrate that granzyme B (GrB)-Fc-KS49, a novel immuno-oncology therapy comprised of the active GrB fused to the immunoglobulin G heavy chain (Fc) domain containing a single-chain antibody against EMP2, may reshape the tumor microenvironment by altering macrophage recruitment and promoting tumor cell death.

HOW THIS STUDY MIGHT AFFECT RESEARCH, PRACTICE OR POLICY

⇒ These findings encourage the development of GrB-Fc-KS49 as an effective therapy for TNBC.

Conclusions GrB-Fc-KS49 showed high specificity and cytotoxicity towards EMP2-positive cells. In vivo, it reduced tumor burden and increased the recruitment of immune cells into the tumor, suggesting that GrB-Fc-KS49 is a promising therapeutic candidate against BC.

INTRODUCTION

Despite advances in diagnosis and treatment, breast cancer (BC) is still a leading cause of death among women with the 5-year survival rate of patients diagnosed with recurrent disease at only 20%.^{1,2} This situation is particularly dire for women with triple-negative BC (TNBC), an aggressive BC subtype characterized by high recurrence, metastasis, and high mortality rates.^{2,3} While immune checkpoint inhibitors (ICIs) have demonstrated enhanced clinical benefit in advanced solid tumors like melanoma, non-small cell lung cancer, and urothelial carcinoma, a

similar treatment strategy has not been successful for the majority of patients with BC.⁴⁻⁶ However, recent studies suggest that TNBC may be among the BC subtypes that may benefit from immunotherapy approaches, given its expression of programmed death-ligand 1 (PD-L1) and a higher proportion of tumor-infiltrating lymphocytes compared with other BC subtypes.^{7,8} Although Food and Drug Administration-approved for patients with metastatic TNBC, pembrolizumab did not significantly improve overall survival in patients with positive PD-L1-positive disease versus chemotherapy alone.⁹ In the early stage of TNBC, the results were better. The pathological complete response rate within the neoadjuvant setting approached 63% (95% CI: 59.5% to 66.4%) for patients who received pembrolizumab in combination with chemotherapy compared with 56% (95% CI: 50.6% to 60.6%) for patients who received chemotherapy alone. Nonetheless, while initially responsive, the 5-year disease-free survival event rate remains low (11.6%) for high-risk, early disease patients,¹⁰ and acquired resistance to ICI-based therapies remains a clinically emerging, major challenge.¹¹

Epithelial membrane protein-2 (EMP2) is a tetraspan protein that mediates the formation and integrity of multi-receptor lipid raft microdomains on the cell membrane, and dysregulation of EMP2 has been shown in a number of gynecologic cancers.¹²⁻¹⁵ While expression of EMP2 is limited in non-pathological breasts, EMP2 expression is increased in greater than 75% of all human BCs sampled relative to normal breast glandular and ductal epithelial cells. High expression was observed in >75% of women with TNBC and in 100% of metastatic lesions.^{12,16} Thus, EMP2 has emerged as a potential target for precision cancer therapeutic approaches.

While antibody-drug conjugates (ADCs) have revolutionized the era of targeted therapy, their potential is yet to be fully realized due to off-target toxicity from drug release and the development of an immunogenic response against the therapeutic agent used.¹⁷⁻¹⁹ Fully human fusion proteins and immunotoxins are an emerging class of therapeutics that represent an innovative approach to the delivery of a deadly payload to a tumor cell with more specificity and potentially fewer avenues for the development of resistance than ADCs. Constructs developed in our laboratory incorporate the serine protease granzyme B (GrB), which has been validated as a cytotoxic payload when delivered as a targeted therapeutically in various formats including ligand-based and single chain antibody.²⁰⁻²⁴

Several features of GrB make it a natural conjugate for immunotoxin therapy. A natural component of the body's defense against viral infection and tumor development, GrB has a well-understood mechanism of action that includes induction of caspase-dependent and independent apoptosis.²⁵⁻²⁷ Unconjugated GrB internalizes into cells in a perforin-dependent manner, significantly limiting off-target toxicity of GrB-based therapies that would be expected with chemotherapeutic agents

delivered by ADCs.²⁸ Further, as GrB is an endogenous protein present in plasma in both normal and pathological states, it is unlikely to engender an immunogenic response.²⁰

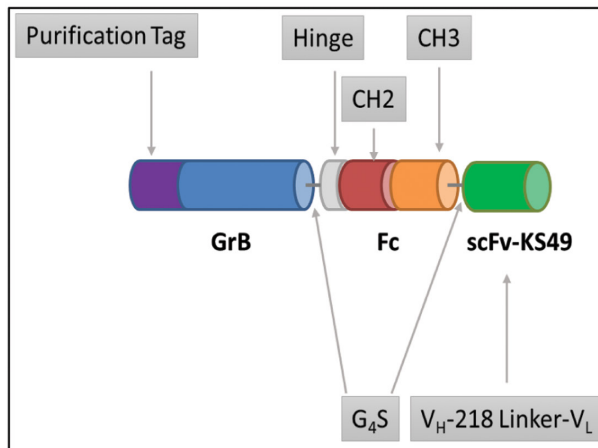
Since GrB is a well-established molecular mediator delivered by cytotoxic T lymphocytes (CTL) and natural killer (NK) cells to target cells, we hypothesized that direct targeting of EMP2+TNBC may simultaneously induce apoptosis of the tumor cell and activate immune cells within the tumor microenvironment (TME). In this study, we developed a novel construct, GrB-Fc-KS49, comprised of the active GrB fused to the immunoglobulin G (IgG) heavy chain (Fc) domain containing a single-chain antibody against EMP2. This new construct showed a high, specific affinity for EMP2 using both flow cytometry and ELISA assays. Moreover, treatment with this agent induced cell death in EMP2-positive cells. Preclinical assessment of GrB-Fc-KS49 showed no acute toxicity and prolonged plasma retention after administration. In vivo efficacy against syngeneic model systems produced a significant reduction in tumor burden and a striking increase in CD45+immunopermissive cells with a notable rebalancing of tumor-associated macrophage (TAM) populations. Our results suggest that continued development of this agent may be successful at targeting advanced BC.

MATERIALS AND METHODS

Cell lines

SKBR3, HEC-1-A, MDA-MB-231, MDA-MB-468, MDA-MB-361, 4T1/_{FLuc} and EMT6 cells were obtained from the American Type Culture Collection (Manassas, Virginia, USA) and cultured for up to 3 months before replacing. BTTR cells are trastuzumab-resistant BT474 cells (kind gift of Neil O'Brien, University of California Los Angeles). All human cells were cultured in Dulbecco's Modified Eagle's Medium (DMEM) medium (Mediatech, Manassas, Virginia, USA) except for HEC-1-A, which was cultured in McCoy's media (MilliporeSigma, St. Louis, Missouri, USA). Both media were supplemented with 10% fetal calf serum (FCS; Hyclone Laboratories, Logan, Utah, USA), 1 mM sodium pyruvate, 2 mM L-glutamine, 100 U/mL penicillin, and 100 U/mL streptomycin (Life Technologies, Carlsbad, California, USA). MEF3.5^{-/-} (MEF3.5) cells are mouse embryo fibroblasts (kind gift of Matthew Hayden, Dartmouth University) and were cultured in DMEM media supplemented with 15% FCS. The endometrial cell line HEC-1-A expressing EMP2 and HEC-1-A KD cells stably expressing a short hairpin RNA (shRNA) lentiviral knockdown of EMP2 were used as controls and have been previously described.²⁹ C8161-GFP cells were a kind gift from Claire Lugassy (Institut Curie, Paris, France). The murine BALB/c syngeneic cells EMT6 and 4T1/_{FLuc} cells were cultured in Roswell Park Memorial Institute medium and supplemented as described above. 4T1/_{FLuc} were stably infected with firefly luciferase (_{FLuc}) as previously described.¹² Cells were cultured in 5% humidified

A



B

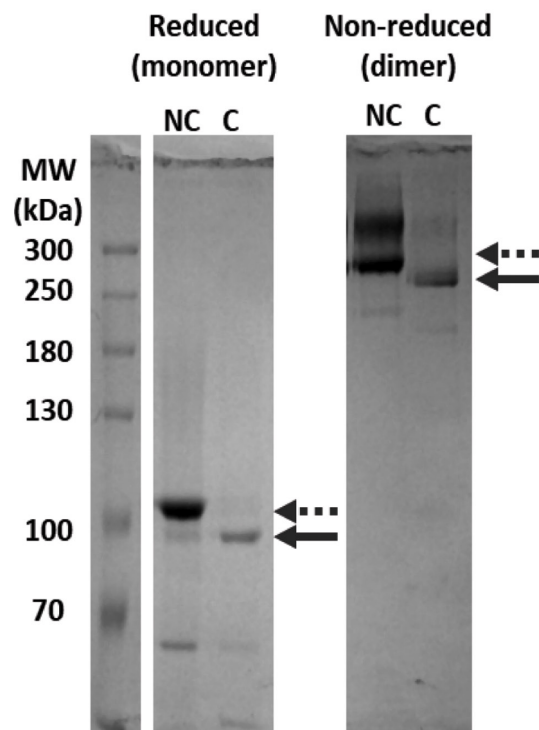


Figure 1 GrB-Fc-KS49 construction and purification. (A) The GrB-Fc-SK49 sequence is preceded by a hexa-histidine tag for purification by metal affinity chromatography, and an enterokinase cleavage site to remove the purification tag and activate granzyme B enzymatic activity. The DNA cassette encoding the GrB-Fc-KS49 sequence was cloned into the mammalian expression vector pSECTag. (B) Purified non-cleaved (dashed arrow) and cleaved (solid arrow) GrB-Fc-KS49 as assessed by SDS-polyacrylamide gel electrophoresis under reduced and non-reduced conditions. C, active GrB-Fc-KS49; GrB, granzyme B; NC, inactive (pro-) form of GrB-Fc-KS49; SDS, sodium dodecyl sulfate.

CO₂ chamber at 37°C. Cells were passaged weekly and tested periodically for mycoplasma contamination using the MycoAlert Kit (Lonza, Hayward, California, USA).

ANIMAL RESEARCH

The work performed was completed under approved protocol # 491-RN03 by the Animal Research Committee at MD Anderson or # 2004-182 by the Animal Research Committee at the University of California, Los Angeles. Experimental details are provided in the online supplemental methods and materials.

Construction of the GrB-Fc-KS49 expression vector

The GrB-Fc-KS49 DNA cassette was generated by overlapping PCR, as previously described.²⁰ The construct is illustrated in figure 1A. Initially, three PCR fragments were generated: Human GrB fused to the N-terminus of the Fc (hinge CH2 and CH3) region of a human IgG1 heavy chain (GrB-Fc), and the previously described variable heavy (VH) and light (VL) sequences for the human anti-EMP2 diabody KS49¹³ flanked by a universal 218 linker, resulting in VH-218 and 218-VL fragments, respectively.²¹ Human GrB can cross-react with other species.³⁰ The fusion construct was completed by two splice overlap

extension PCR reactions, first with VH-218 and 218-VL to generate the VH-218-VL scFv (KS49scFv), followed by GrB-Fc with KS49scFv to generate GrB-Fc-KS49. The cassette was cloned into the mammalian expression vector pSecTag (Life Technologies, Waltham, Massachusetts, USA).

Expression and purification of GrB-Fc-KS49

GrB-Fc-KS49 was expressed in HEK-293E cells, as previously described.^{20, 22} Briefly, cells (9×10⁶ cells/mL) were transiently transfected with a mixture of the expression vector (4.5 µg/mL) with polyethylenimine (1:4.5) for 4 hours. Cells were diluted 1:1 with growth media and grown overnight at 37°C and 120 rpm. Following the addition of 3.8 mM valproic acid and 1:1000 anti-clumping agent, cells were incubated for a further 72 hours prior to harvesting the conditioned media, which contained the inactive (pro-) form of GrB-Fc-KS49. After purification of the dimer by cobalt-metal affinity chromatography, the protein was activated by cleavage of the purification tag with recombinant enterokinase (20 U/mg).²⁴ Further purification by SP Sepharose chromatography to remove the cleaved tag resulted in purified, active GrB-Fc-KS49.

Additional methods are described in the online supplemental methods and materials.

RESULTS

GrB-Fc-KS49 expression and purification

Immunotoxins are antibody-toxin bifunctional molecules that combine the specificity of an antibody with a potent intracellular payload to kill target cells. We have previously characterized diabodies to EMP2 which show specificity and sensitivity to its expression. To create a second generation of molecules targeting EMP2, we fused the KS49 scFv with GrB as a toxin payload to ultimately determine its therapeutic efficacy (figure 1A). One liter of HEK-293E conditioned medium yielded approximately 20 mg of purified GrB-Fc-KS49 protein. Sodium dodecyl sulfate-polyacrylamide gel electrophoresis (SDS-PAGE) analysis showed one band at ~250 kDa and 100 kDa under non-reducing and reducing conditions, respectively,

clearly demonstrating that the final construct is present as a disulfide-linked dimer as expected (figure 1B). Comparison of GrB-Fc-KS49 with its expected dimeric molecular weight of ~158 kDa suggests significant glycosylation when produced in HEK-293E cells.

Assessment of cellular EMP2 levels

We have previously shown that EMP2 is expressed in many human and murine breast and endometrial cancer cell lines.^{29 31} Within different subtypes, EMP2 is expressed in both hormone receptors, HER2+positive, as well as in TNBC. Western blot analysis indicated a range of cellular EMP2 expression (figure 2A), with all BC cell lines tested showing moderate to high levels of EMP2 expression. The highest EMP2 levels were observed in the human HER2+BC cell lines MDA-MB-361 and SKBR3 and the mouse TNBC cell line 4T1/_{FLuc}. The human TNBC cell line MDA-MB-468 also showed high expression of EMP2. Two additional cell lines, the human melanoma

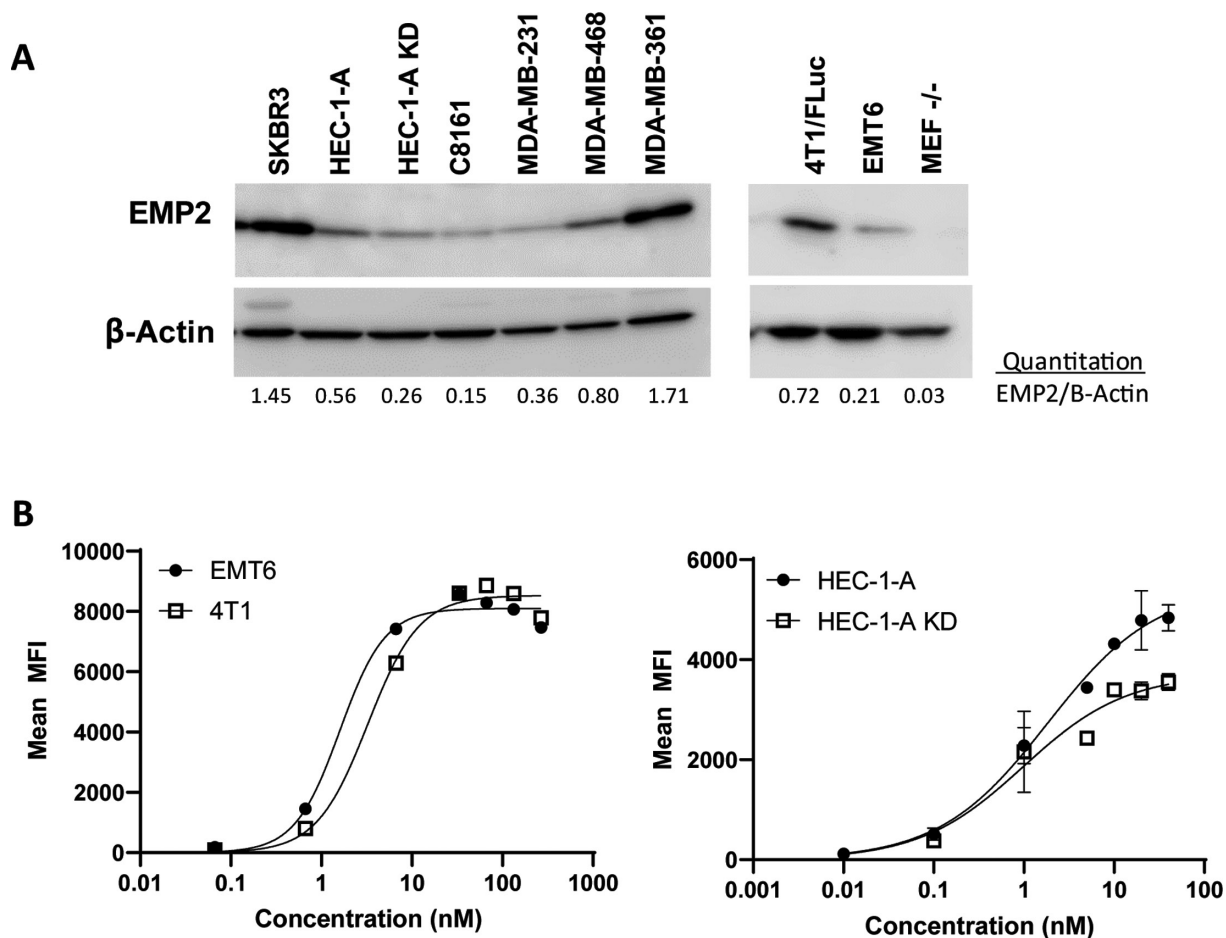


Figure 2 Validation of binding characteristics of the GrB-Fc-KS49 immunotoxin to EMP2 cells. (A) Left, EMP2 expression in a panel of breast cancer cells was compared with the endometrial cancer cell line HEC-1-A and the melanoma cell line C8161 in a panel of human cells. Right, the level of EMP2 expression was measured in the murine 4T1/_{FLuc}, EMT6 and MEF cells. (B) Left, binding of the immunotoxin to 4T1/_{FLuc} and EMT6 cells show similar surface expression of the EMP2 antigen. The experiment was performed three times, with one representative experiment shown. The Kd was calculated using non-linear regression with specific binding. Right, surface binding of the GrB-Fc-KS49 immunotoxin to EMP2 was measured in HEC-1-A cells or cells engineered to stably express a shRNA lentiviral knockdown vector (HEC-1-A KD). Results are the average of two independent experiments, with error bars indicating SEM. EMP2, epithelial membrane protein-2; shRNA, short hairpin RNA. Kd, equilibrium dissociation constant. MFI, mean fluorescence intensity.

cell C8161-GFP as well as murine embryonic fibroblasts MEF3.5 expressed low to undetectable levels of EMP2. For comparison, expression was also measured in the endometrial cancer cell line HEC-1-A, with the specificity of the response confirmed using the HEC-1-A shRNA knockdown cell line HEC-1-A KD.

Binding affinity of GrB-Fc-KS49

To confirm that the scFv portion of GrB-Fc-KS49 immunotoxin recognized EMP2, we first determined the binding affinity of GrB-Fc-KS49 by Octet binding. Using a 1:1 binding model, the GrB-Fc-KS49 immunotoxin showed a strong equilibrium affinity constant (Kd) of 1×10^{-12} M to an EMP2 peptide with no significant binding to a non-specific control (online supplemental figure S1). Next, we sought to confirm the specificity of the GrB-Fc-KS49 immunotoxin to cell surface EMP2 on cell lines with validated EMP2 levels using flow cytometry. The correlation of cellular EMP2 levels to cell surface expression levels was validated by demonstrating high cell surface binding of GrB-Fc-KS49 to two murine TNBC lines EMT6 and 4T1_{FLuc}. While 4T1_{FLuc} cells showed increased total EMP2 expression, both cell lines showed similar binding and saturation levels, suggesting that they may have a similar surface expression of the antigen. The calculated Kd for the GrB-Fc-KS49 were 2.063 ± 0.35 and 1.469 ± 0.89 nM for EMT6 and 4T1_{FLuc}, respectively, which is similar to binding from the KS49 IgG1.³² Binding was also tested on the HEC-1-A cell line which was used as a positive control as well as on cells engineered to knock-down EMP2 expression in HEC-1-A KD (figure 2B). While the Kd was similar for HEC-1-A and HEC-1-A KD (1.3 vs 1.0 nM, respectively), the calculated maximum number of binding sites or Bmax showed the expected reduction, going from 5462 to 3716 for the two cell lines, respectively. Thus, GrB-Fc-KS49 appears to be an excellent candidate to target EMP2 on TNBC cells and other EMP2+ cancers.

GrB activity assay

Our results thus far demonstrated that the binding of the GrB-Fc-KS49 immunotoxin was dependent on EMP2 levels. Next, an enzymatic activity assay was performed to evaluate the activity of the GrB component. The specific activity of commercial GrB was 122 ± 10 U/nmol, and that of GrB-Fc-KS49 ranged from 98 ± 5 U/nmol GrB ($p=0.08$, Student's t-test) indicating that while some GrB enzymatic activity is lost, the molecule retained a high degree of its enzymatic function within the fusion construct (online supplemental figure S2).

Cytotoxicity of GrB-Fc-KS49 in vitro

The in vitro cytotoxicity of GrB-Fc-KS49 was assessed against a panel of BC and control cell lines (table 1 and online supplemental figure S3). Using an endometrial cancer cell line as a positive control, HEC-1-A was sensitive to GrB-Fc-KS49 treatment in vitro, with an average half-maximal cytotoxicity (IC₅₀) of 44 ± 5 nM. HEC-1-A KD cells with downregulated EMP2 were ~4-fold less sensitive, indicating that the cytotoxicity of the GrB-Fc-KS49 was receptor-mediated. The IC₅₀ of the GrB-Fc-KS49 construct ranged from 40 to 83 nM against all tested human and mouse TNBC cell lines as well as the HER-2+ cell line SKBR3. In contrast, cell lines with very low to undetectable EMP2 levels were less sensitive to GrB-Fc-KS49. For all cells, free GrB had low cytotoxicity, indicating that the cytotoxicity is driven by the construct. Because internalization of antibodies and fusion proteins can result in their entrapment in the endo/lysosomal compartments and result in diminished cytotoxicity, we examined the effect of chloroquine, a known lysosomotropic agent, on cytotoxicity against MDA-MB-231 cells.²¹ A cytotoxicity profile of various concentrations of chloroquine against MDA-MB-231 cells established an IC₅₀ of approximately 50 μM over 72 hours (online supplemental figure S3B) and 10 μM as the minimal level required to demonstrate

Table 1 Cytotoxicity of GrB-Fc-KS49 on various cell lines

Category	Cell line	Cell type	Species	EMP2 receptor sites per cell	IC ₅₀ (nM) GrB-Fc-KS49	IC ₅₀ (nM) granzyme B
Breast cancer cell lines	MDA-MB-468 (log-phase)	Breast	Human	++	40±7	704±58
	MDA-MB-231	Breast	Human	++	64±4	3,881±1,176
	MDA-MB-231*	Breast	Human	++	82±8	ND
	SKBR3	Breast	Human	+++++	83±3	4,373±343
	EMT6	Breast	Mouse	+++	71±3	ND
	4T1 _{FLuc}	Breast	Mouse	++++	82±2	6,159±593
Control cell lines	HEC-1-A	Endometrial	Human	+++	44±5	>5,000
	HEC-1-A KD	Endometrial	Human	+	169±22	>600
	C8161-GFP	Melanoma	Human	-	2,822±124	ND
	MEF3.5 -/-	Fibroblast	Mouse	-	441±4	>600

*Treatment in the presence of 10 μM chloroquine.
EMP2, epithelial membrane protein-2; GrB, granzyme B; IC₅₀, half-maximal cytotoxicity; ND, not determined.

toxicity. The presence of 10 μ M chloroquine in combination with GrB-Fc-KS49 did not improve cytotoxicity towards these cells (table 1), suggesting that GrB-Fc-KS49 is efficiently released from intracellular vesicles and can access cytosolic GrB substrates.

Internalization of GrB-Fc-KS49 into TNBC cells

We assessed the internalization of GrB-Fc-KS49 by immunofluorescence microscopy. The fusion protein internalized within 4 hours in the EMP2+BC cell lines, while internalization of the untargeted GrB was not observed, suggesting receptor-mediated internalization (online supplemental figure S4). To confirm its specificity to EMP2-positive cells, internalization of GrB-Fc-KS49 or GrB was also evaluated in MEF3.5 cells. No internalization was observed in this cell line.

Effects of GrB-Fc-KS49 on clinical chemistry parameters

Clinical chemistry parameters tested at 40 mg/kg GrB-Fc-KS49 delivered over 2 weeks were evaluated in CD-1 mice. Interestingly, whereas an increase in alkaline phosphatase (ALP) is indicative of toxicity,³³ the levels of ALP showed a slight but significant decrease in GrB-Fc-KS49 treated mice. Nonetheless, ALP levels in both control and GrB-Fc-KS49 treated mice fall within the serum chemistry reference range for CD-1 mice.³⁴ For all other parameters tested, a comparison of the control versus GrB-Fc-KS49 treated mice showed no significant alterations, suggesting a lack of toxicity associated with the GrB construct (table 2).

Ex vivo stability and in vivo pharmacokinetics

The relative stability of GrB-Fc-KS49 under ex vivo conditions was assessed using sterile mouse serum at 37°C for 96 hours. As shown in figure 3A, Western blot analysis indicated a gradual reduction in GrB-Fc-KS49 over time. Quantitation of the SDS-PAGE gel by densitometric analysis of the Western blots indicated that GrB-Fc-KS49 was relatively stable at 37°C in mouse serum with an overall half-life exceeding 96 hours (figure 3B). Next, we determined the pharmacokinetics (PK) of the GrB-Fc-KS49 immunotoxin in vivo by injecting mice with the GrB-Fc-KS49 and assessing the Fc portion of the immunotoxin using Western blot analysis. In vivo PK indicated a biexponential plasma clearance, with a moderate initial clearance ($t_{1/2\alpha}$ =18.4 hours) and a much slower terminal clearance rate ($t_{1/2\beta}$ =73.1 hours), confirming that GrB-Fc-KS49 is stable in vivo (figure 3C). The drug concentration at time 0 was determined to be 156 μ g/mL. The volume of distribution was a relatively low 2.58 mL, suggesting the limited distribution of GrB-Fc-KS49 into peripheral sites outside the vasculature immediately after administration.

In vivo efficacy

To next evaluate the efficacy of GrB-Fc-KS49, syngeneic orthotopic models were created using 4T1/_{FLuc} cells. When tumors approached 100 mm³, they were treated with the immunotoxin or control IgG two times per week. Treatment with GrB-Fc-KS49 significantly reduced tumor load (p =0.002, figure 4A; Online supplemental figure S5A), and throughout the treatment period, no

Table 2 Toxicity profile of GrB-Fc-KS49 compared to the vehicle control. N=4/group

	Vehicle control	GrB-Fc-KS49	P value
Total bilirubin (mg/dL)	<0.15	<0.15	ND
Albumin (g/dL)	3.63±0.17	3.62±0.03	0.96
ALP (U/L)	143.25±39.99	92±10.17	0.049
ALT (U/L)	150.25±74.28	92.25±21.06	0.19
AST (U/L)	1,268.75±662.88	717.25±247.42	0.17
BUN (mg/dL)	23.7±4.39	25.08±2.19	0.61
Calcium (mg/dL)	9.1±0.08	9.38±0.24	0.10
Chloride (mEq/L)	109.5±2.38	110.75±1.79	0.46
Creatinine (mg/dL)	0.29±0.09	0.255±0.24	0.48
Globulin (g/dL)	1.19±0.40	0.97±0.10	0.34
Potassium (mEq/L)	9.43±1.88	7.93±0.41	0.17
LDH (U/L)	5,297.5±2,368.2	2,982.75±524.27	0.11
Sodium (mEq/L)	145±2.16	146.25±0.83	0.33
Phosphorus (mg/dL)	9.88±1.33	9.0±0.47	0.27
Glucose (mg/dL)	139±26.09	162.75±15.79	0.19
Total protein (g/dL)	4.81±0.46	4.59±0.13	0.40

ALP, alkaline phosphatase; ALT, alanine transaminase; AST, aspartate transaminase; BUN, blood urea nitrogen; GrB, granzyme B; LDH, lactate dehydrogenase; ND, not determined.

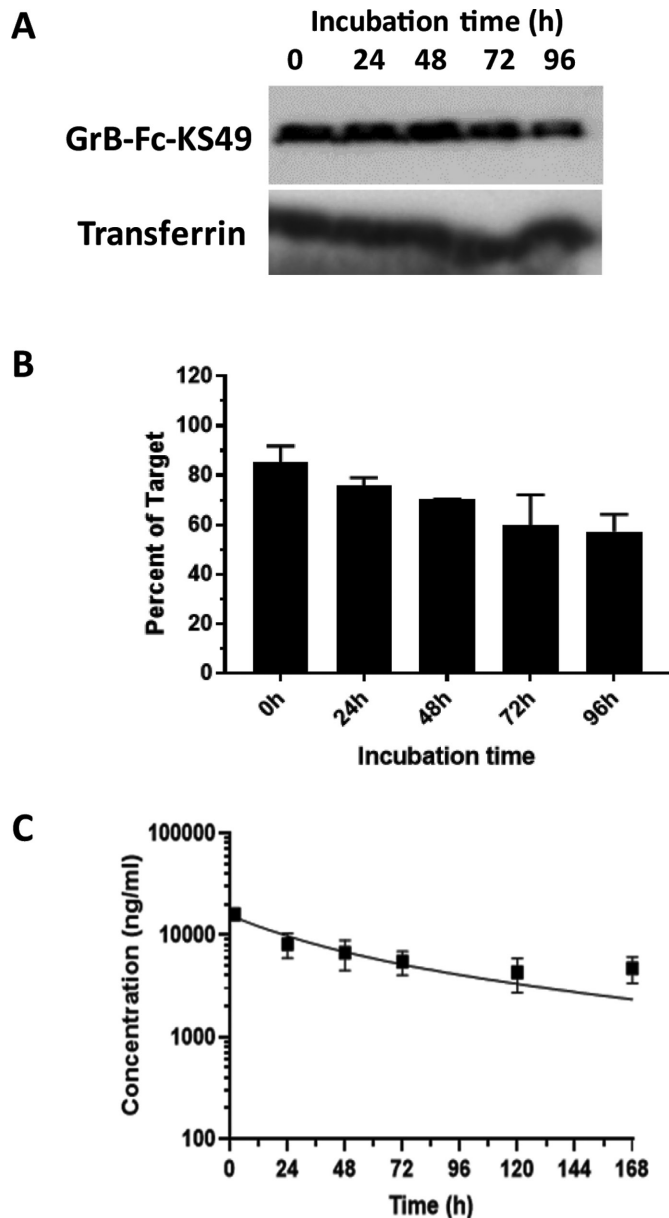


Figure 3 Ex vivo serum stability and in vivo pharmacokinetics. (A) Stability of GrB-Fc-KS49 in mouse serum at 37°C was assessed by Western blot (representative blot shown). (B) The Western blots were quantitated by densitometric analysis. The overall half-life of GrB-Fc-KS49 exceeded 96 hours. Data represents the average from four mice, with error bars indicating SEM. (C) In vivo pharmacokinetics of the GrB-Fc-KS49. Injection of 400 µg of GrB-Fc-KS49 indicated a two-phase clearance with a $t_{1/2\alpha}$ of 18.4 hours and a $t_{1/2\beta}$ of 73.1 hours. GrB, granzyme B.

signs of animal toxicity were observed (online supplemental figure S5B). This included no signs of chronic pain (eg, reluctance to move or failure to groom) as well as no changes in appetite as evaluated by fluctuations in weight (online supplemental figure S5B). To evaluate the histology of the tumors, they were initially fixed and analyzed by H&E, and increased cell death and immune infiltrates were observed (figure 4B and online supplemental figure S5C). To confirm these features, we

stained the tumors for Ki-67 expression and performed the terminal deoxynucleotidyl transferase dUTP nick end labeling (TUNEL) assay to assess tumor cell proliferation and cell death, respectively. Compared with the control treatment, GrB-Fc-KS49 reduced cellular proliferation as measured by Ki-67 expression by more than twofold ($p=0.001$; figure 4C, top). To next distinguish necrosis from apoptosis within these specimens, we performed a TUNEL assay.³⁵ Samples were stained using the TUNEL kit to detect DNA strand breaks (fluorescein isothiocyanate; FITC) and Isolectin GS-IB4 Alexa Fluor 594 to assess vascular changes (figure 4C, bottom; higher magnification images are provided in online supplemental figure S5D). Compared with the control, treatment with the GrB-Fc-KS49 immunotoxin significantly enhanced cell death while reducing the presence of tumor-associated vasculature ($p=0.02$).

GrB-Fc-KS49 treatment increases tumor infiltration of CD45+ cells

Traditionally, breast tumors are considered immunologically quiescent,³⁶ but post-GrB-Fc-KS49 treatment, an altered histological distribution could be observed. To confirm that these cells were of immune origin, tissue sections were stained using anti-CD45 antisera. GrB-Fc-KS49 treatment significantly increased the percentage of CD45+ cells within the tumor ($p=0.003$, figure 4D, top). Within the TME, TAMs have been reported to be the most abundant immune cells, and these cells have been shown to regulate BC regression or progression through their ability to polarize into proinflammatory M1 macrophages or immunosuppressive M2 macrophages, respectively.^{37,38}

It has been reported that macrophages exist in high numbers at the margins of breast tumors but decrease within the tumor stroma.^{38,39} Within the tumor, macrophages may be found in association with blood vessels where they are believed to help orchestrate the migration of tumor cells.⁴⁰ To evaluate M1 and M2 macrophages within these 4T1/_{FLuc} tumors, we stained tumors for iNOS to detect M1 macrophages or CD206 to evaluate M2 macrophages. While M1 macrophages were typically present at low numbers throughout the tumor, GrB-Fc-KS49 significantly increased the number of cells observed per field ($p=0.0006$, figure 4D, middle panel). In contrast, M2 macrophages were readily observed along the periphery of control tumors, but these numbers were reduced with immunotoxin treatment ($p=0.01$, figure 4D, bottom panel).

GrB-Fc-KS49 treatment of EMT6 xenografts significantly increases immunopermissive M1 TAMs around the tumor vasculature

To validate these effects, we created a second TNBC syngeneic model using EMT6 cells. Treatment with GrB-Fc-KS49 began 1 week after tumor placement (50–100 mm³) with GrB-Fc-KS49 or with control IgG administered intraperitoneally two times per week. As in the previous model, the study was terminated 2 weeks after onset of treatment,

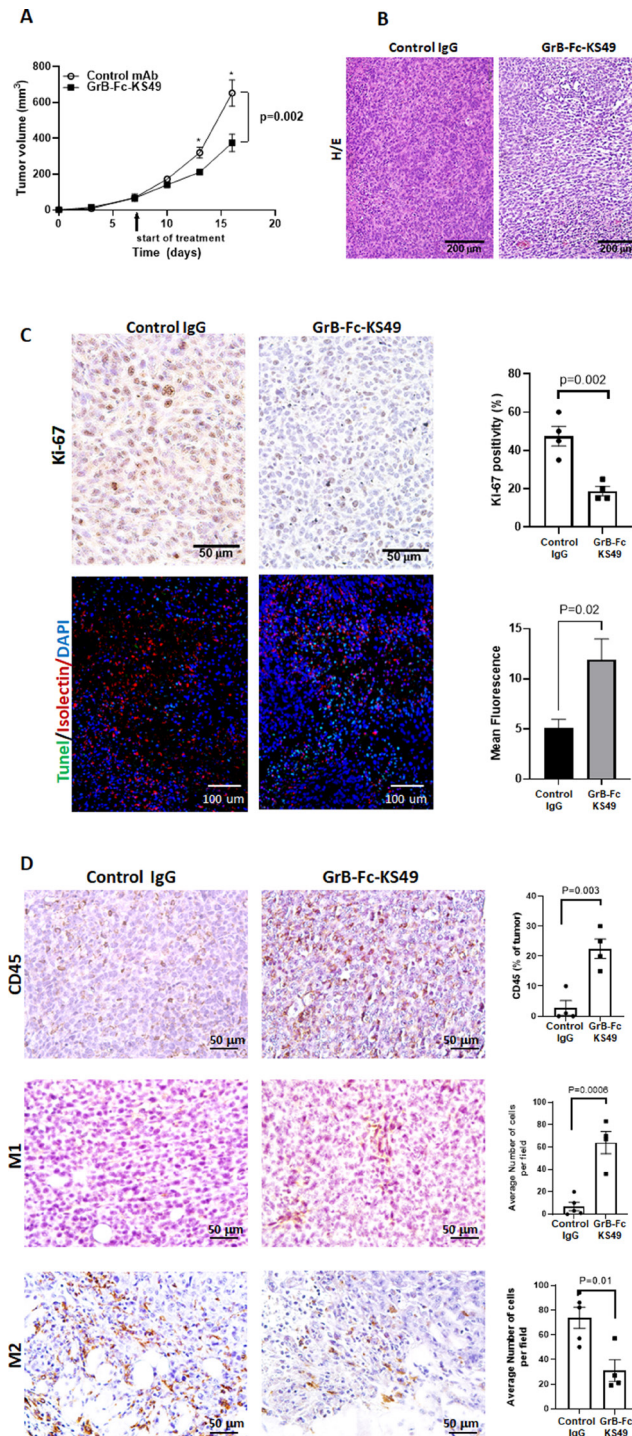


Figure 4 GrB-Fc-KS49 treatment reduces tumor load in a 4T1/_{FLuc} breast cancer model. (A) 4T1/_{FLuc} cells were implanted in the mammary fat pad of BALB/c animals. Tumors (50–100 mm³) were treated 3 times over 10 days with control IgG or the GrB-Fc-KS49 immunotoxin at 10 mg/kg. Results are expressed as the mean±SEM from n=4 for control or n=5 GrB-Fc-KS49 groups, and statistical differences are determined using a two-way ANOVA with Bonferroni's multiple comparison test used for post hoc analysis. *p<0.05. (B) Tumor histology was evaluated on FFPE tumor sections using H/E staining. (C) For each group, all tumors were also stained for Ki-67 as a measure of cellular proliferation, with quantitation of staining presented to the right. All tumors were also stained by the TUNEL assay to measure apoptosis (FITC), Isolectin GS-IB4 Alexa Fluor 594 to assess vascular changes, and counterstained with DAPI. n=4 with results expressed as the mean±SEM. Statistical differences were determined using Student's t-test. (D) Immunohistochemical staining of tumors for CD45, iNOS (M1 macrophage marker), and CD206 (M2 macrophage marker). Representative 400× magnification images are shown with quantitation of staining to the right. n=4 with results expressed as the mean±SEM. Statistical differences were determined using Student's t-test. ANOVA, analysis of variance; DAPI, 4',6-diamidino-2-phenylindole; FFPE, formalin-fixed paraffin-embedded; FITC, fluorescein isothiocyanate; GrB, granzyme B; IgG, immunoglobulin G; mAb, monoclonal antibody; TUNEL, terminal deoxynucleotidyl transferase dUTP nick-end labeling.

due to the control group tumors approaching 1500 mm³. Treatment with the immunotoxin reduced tumor load by twofold over the short duration of the study ($p=0.03$; [figure 5A](#)). The growth rate from individual mice is shown in online supplemental figure S6A). Similar to the 4T1/_{FLuc} study, these tumors exhibited marked cellular death and immune infiltration by standard H&E staining ([figure 5B](#) and online supplemental figure S6B). We next analyzed the tumors by immunohistochemistry to probe for EMP2 expression, tumor proliferation, and immune composition. EMT6 strongly expresses EMP2 in a cytoplasmic/membrane distribution, and treatment with the GrB-Fc-KS49 showed a slight, non-significant reduction in expression ([figure 5C](#), top panel). We next examined Ki-67 expression as an estimate of tumor growth and used the TUNEL assay to evaluate cell death. Treatment with GrB-Fc-KS49 significantly reduced Ki-67 expression ($p=0.005$, [figure 5C](#), middle panel) while samples stained by TUNEL (FITC) and Isolectin GS-IB4 Alexa Fluor 594 showed DNA strand breaks and vascular changes, respectively. Treatment with the GrB-Fc-KS49 immunotoxin relative to the control showed significantly more positive staining by TUNEL while reducing the presence of tumor-associated vasculature ($p=0.02$; [figure 5C](#), bottom). Higher magnification images are shown in online supplemental figure S6C).

As in the study with 4T1/_{FLuc} tumors, EMT6 tumors showed notable cytologic heterogeneity. To characterize these cells, tumors initially were stained for CD45 to evaluate the immune composition within the microenvironment. GrB-Fc-KS49 treated cells showed a significant increase in CD45+cells compared with control-treated tumors ($p=0.002$, [figure 5D](#), top panel). Within this population of immune cells, we characterized the TAMs and found a significant increase in M1 macrophages within the immunotoxin-treated tumor, particularly concentrated around tumor vasculature ([figure 5D](#), middle panel). In contrast, along the periphery of the tumor, a reduction in M2 macrophages as measured by CD206 expression was observed ([figure 5D](#), bottom panel). These results collectively suggest that GrB-Fc-KS49 alters the TME and may allow it to become more immune-permissive.

Immunotoxin-treated animals show an upregulation in immune signatures compared with control animals

To validate and further understand how the immunotoxin altered the TME, we performed RNA sequencing of whole tumor tissues on EMT6 tumors treated with either a control antibody or the GrB-Fc-KS49 immunotoxin as above. In these experiments, to limit ulceration, treatment ceased when tumors approached 1000 mm³. Similar to the results presented above, EMT6 tumors showed a reduction in tumor load when treated with the immunotoxin (online supplemental figure S7A). Initial exploration of whole-transcriptome data revealed expected variations in cell-type composition across samples as estimated through deconvolution analysis (see online supplemental methods). These variations are common

confounding factors in the analysis of the tumor transcriptomics.⁴¹ To minimize the effect of cellular heterogeneity in our analyses, we regressed out the estimated TME scores from the gene expression matrix (see online supplemental methods). As a result, the main sources of gene expression variability in the corrected data fully segregated the control and GrB-Fc-KS49 treated samples (online supplemental figure S7B), and this transformed data was used for all downstream analysis (online supplemental figures S6–S8).

We first unitized gene set enrichment analysis to evaluate the macrophage signature in immunotoxin versus control-treated tumors. Analysis revealed an increased score in canonical macrophage expression after treatment with the immunotoxin, and this increase was mostly associated with a preferential M1 signature (online supplemental figure S7C) in GrB-Fc-KS49-treated samples as compared with control samples. More specifically, we next evaluated the ratio of M1:M2 macrophages using the NOS2:Mrcl (iNOS:CD206) ratio and cellular proliferation using murine Ki-67 expression following treatment with the GrB-Fc-KS49 immunotoxin or control ([figure 6A](#)). In agreement with the immunohistochemistry results presented above, treatment with the GrB-Fc-KS49 immunotoxin induced a significant reduction in mKi-67 expression. M1 and M2 macrophages are often defined by multiple markers such as CD86, CD80, and iNOS for M1 macrophages or Arg1 and CD206 for M2 macrophages. To evaluate if the immunotoxin produced a consistent effect, we examined its ability to affect the M1 and M2 ratio across these markers. The GrB-Fc-KS49 immunotoxin increased the ratio of M1 to M2 macrophages when evaluating CD86:Arg1 or CD80:Arg1 levels (online supplemental figure S7D).

Further differential expression analysis between the GrB-Fc-KS49 treatment and control revealed a small yet distinct set of significantly regulated genes (empirical Bayes t-test p value <0.05 , [figure 6B](#)). In fact, functional enrichment of genes upregulated by the immunotoxin revealed a signature of inflammation and adaptive immune response pathways ([figure 6C](#)) while genes downregulated after GrB-Fc-KS49 treatment control-treated tumors showed enrichment in genes associated with chemical homeostasis and positive regulation of vascular associated smooth muscle cell migration, among others ([figure 6C](#), online supplemental figure S8). Specifically, 9 of the top 20 significantly regulated genes were involved in the regulation of inflammatory cells including dendritic cells (Siglech), B cells (Spib, CD22) and NK cells (Kird1) ([figure 6D](#)). In addition, genes involved in caspase-dependent cell death were upregulated (Rabac1), while genes in pathways associated with tumor progression were downregulated (Sema3c, Osmr, Plekhh2, Dclk1).

DISCUSSION

In BC, our previous results have shown that EMP2 is upregulated in over 75% of patients, including those with

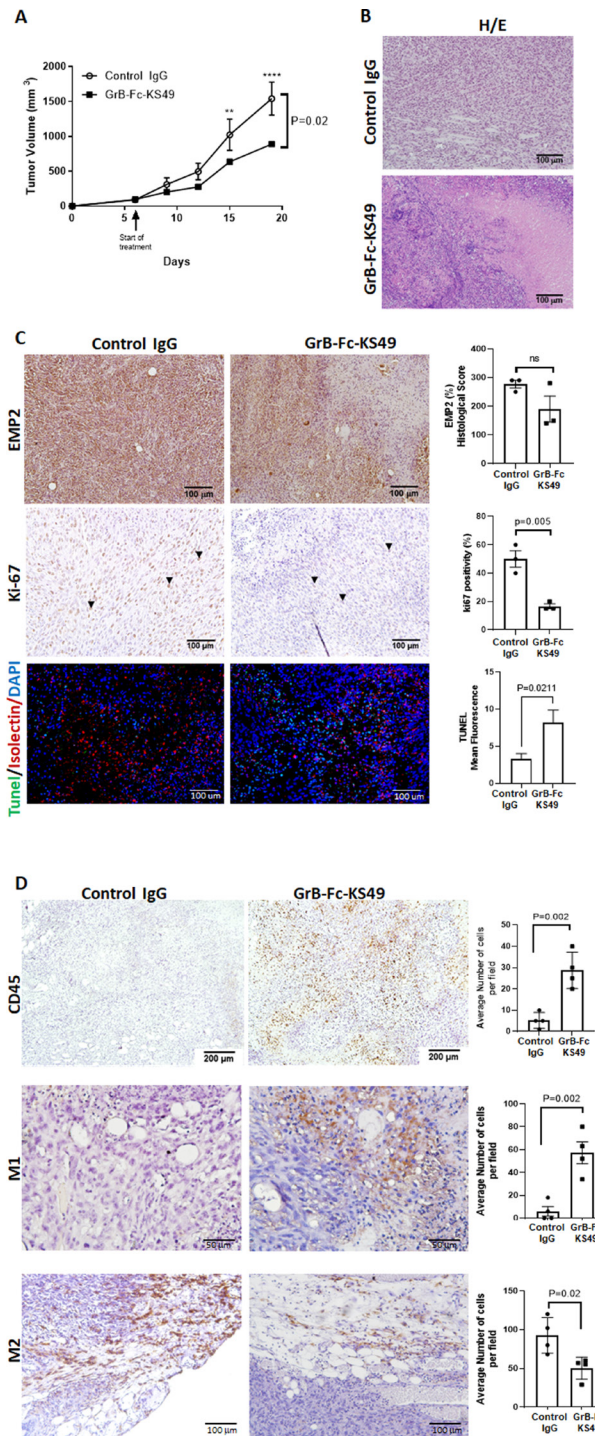


Figure 5 GrB-Fc-KS49 treatment improves survival in the EMT6 breast cancer model. (A) EMT6 cells were implanted in the mammary fat of BALB/c animals. Tumors (50–100mm³) were treated two times per week with control IgG or the GrB-Fc-KS49 immunotoxin at 10mg/kg. Average tumor load±SEM is shown from n=5 control or n=5 GrB-Fc-KS49 groups. Statistical differences were determined using a two-way ANOVA with Bonferroni's multiple comparison test used for post hoc analysis. *p<0.05. (B) Tumor histology was evaluated on FFPE tumor sections using H&E staining. Images from a representative tumor from each group are shown. (C) For each group, all tumors were also stained for EMP2 and Ki-67 with representative images shown. Samples were also stained by the TUNEL assay (FITC), Isolectin GS-IB4 Alexa Fluor 594, and nuclei counterstained with DAPI, with a representative image shown. Quantitation of staining is shown to the right. n=3 with results expressed as the mean±SEM. Statistical differences were determined using an unpaired Student's t-test. (D) Immunohistochemical staining of tumors for CD45, iNOS (M1 macrophage marker) and CD206 (M2 macrophage marker). Representative images at the indicated magnifications are shown with quantitation of staining to the right. n=4 with results expressed as the mean±SEM. Statistical differences were determined using an unpaired Student's t-test. ANOVA, analysis of variance; DAPI, 4',6-diamidino-2-phenylindole; EMP2, epithelial membrane protein-2; FFPE, formalin-fixed paraffin-embedded; FITC, fluorescein isothiocyanate; GrB, granzyme B; IgG, immunoglobulin G; TUNEL, terminal deoxynucleotidyl transferase dUTP nick-end labeling.

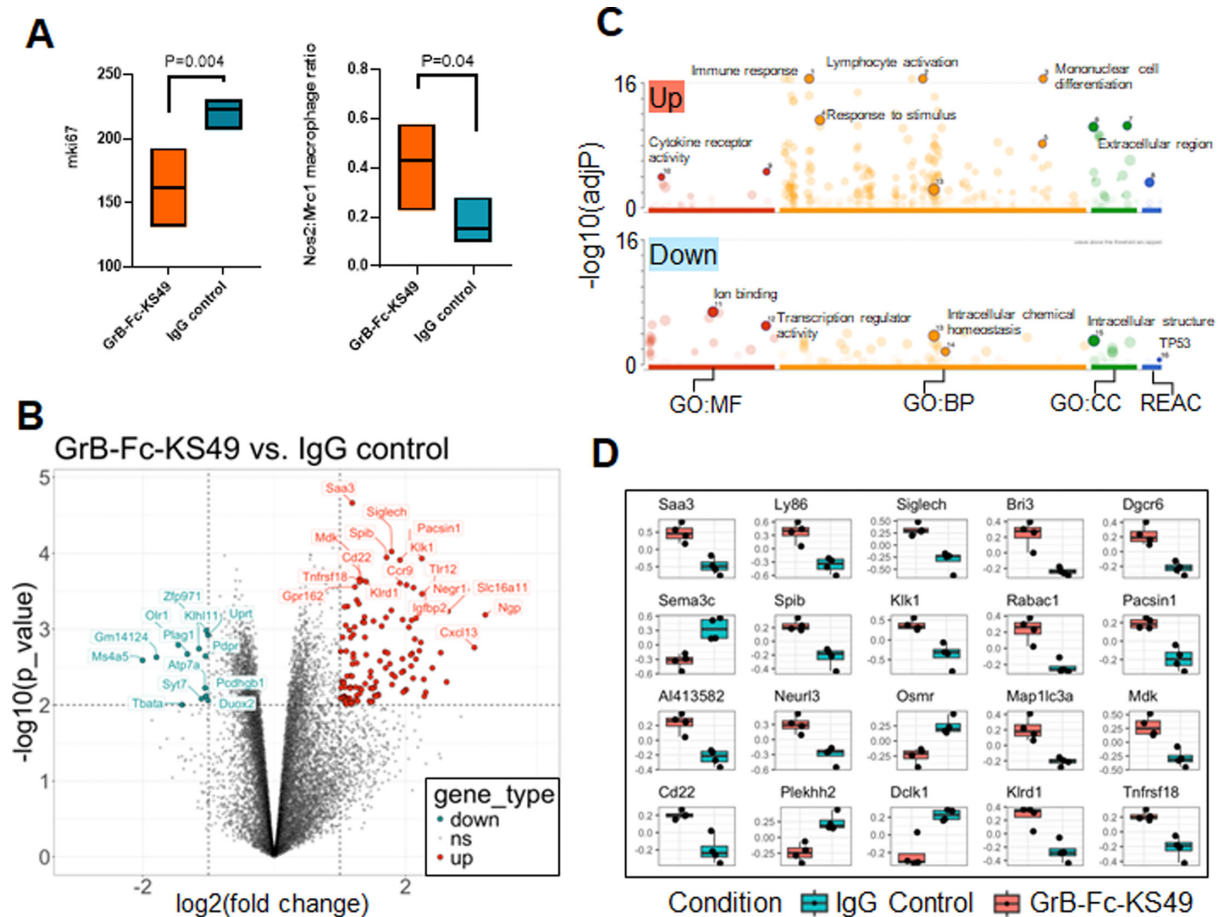


Figure 6 GrB-Fc-KS49 increases immune infiltration within the tumor microenvironment. (A) Estimated gene expression of the proliferation marker mKi67 (left) and expression ratio of M1 (Nos2 or iNOS) and M2 (Mrc1 or CD206) macrophage markers (right) for the control and immunotoxin-treated mice (from RNA-seq data). (B) Volcano plot summarizing RNA-seq differential expression results between immunotoxin and control IgG-treated tumors. Selected genes identified as significantly regulated are highlighted. Upregulated genes correspond to those showing higher expression after treatment with the GrB-Fc-KS49 immunotoxin. Key: down (downregulated), ns (not significant), up (upregulated). (C) Functional enrichment of upregulated and downregulated genes. Selected, non-redundant pathways are highlighted. Key: GO:MF (Gene Ontology, Molecular Function); GO:BP (Gene Ontology Biological Processes), GO:CC (Gene Ontology Cellular Component); REAC (Reactome Pathways). (D) Expression barplots for the top 20 most significant genes between immunotoxin and control IgG-treated tumors (empirical Bayes t-test p value, from RNA-seq data, n=4 per group). The y-axis represents the gene expression residuals after correcting for the estimated tumor heterogeneity (see online supplemental methods). GrB, granzyme B; IgG, immunoglobulin G.

the triple-negative subtype. Loss of EMP2 reduces tumor growth, in part likely due to its regulation of HIF1 α and tumor-mediated neoangiogenesis.³¹ We have previously created diabodies to EMP2 and shown that they have the potential to internalize.¹⁶ In this study, we aimed to improve and optimize recombinant scFv fragments for targeted therapy by creating an immunotoxin.⁴² Immunotoxins make up a category of protein-based therapeutics. They typically consist of at least two domains, where one part allows for receptor binding and the other part induces apoptosis after internalization.

GrB is a well-known serine protease that is part of the body's natural defense against viral infection and tumor development, delivered by CTL and NK cells to the target cells.²⁵ Once endocytosed, GrB remains trapped in endocytic vesicles until released by perforin into the cytosol, where it induces caspase-dependent and independent apoptosis, as well as directly cleaving nuclear matrix

material.²⁷ Capitalizing on this ability, we developed a fully human GrB-based immunotoxin to the tetraspan protein EMP2 termed GrB-Fc-KS49. In this study, we characterized its ability to bind to human and murine EMP2 as we have previously shown that this scFv cross-reacts to both species.^{43 44} Like those studies, the immunotoxin to EMP2 displayed sensitivity to EMP2 levels in both mouse and human cell lines, and this specificity translated to its internalization and subsequent apoptosis of EMP2-positive cells. This phenotype was further observed in vivo, where in both EMT6 and 4T1/_{FLuc} syngeneic models, treatment with the GrB-Fc-KS49 reduced tumor load and increased immune cell recruitment to the tumor.

To begin its preclinical characterization, the immunotoxin was evaluated for both its PK and for acute toxicity as we and others have documented that EMP2 is expressed in type I pneumocytes of the lung as well as in keratinocytes of the epidermis.^{16 45 46} Preliminary characterization

revealed no visible toxicity or death in animals, suggesting that the 10 mg/kg dosage is well tolerated. To evaluate the PK of the immunotoxin, we evaluated its presence through the detection of the Fc region and binding to an EMP2 peptide. Our studies show an initial clearance of $t_{1/2\alpha}$ of 18.4 hours and a much slower terminal $t_{1/2\beta}$ of 73.1 hours, which is in line with other GrB-immunotoxins published.^{20 22}

While we did observe significant efficacy of GrB-Fc-KS49 *in vivo*, the overall length of each study was limited primarily due to the growth rate of control tumors. Given that the doses of other GrB-based constructs in our studies exceed doses administered here by at least threefold, it is likely that efficacy can be markedly improved by this construct at higher doses.²⁰ While the maximum tolerated dose of GrB-Fc-KS49 has not yet been established, an increased dose at this schedule is unlikely to result in toxicity as doses of GrB-based therapeutics approaching 500 mg/kg (over 10 times the total dose used in these studies) have been shown to be non-toxic (manuscripts in preparation). In addition, our recent studies with other GrB-based constructs have shown that a weekly dose schedule (QW×5) improves efficacy compared with schedules with shorter intervals.²⁰ Studies are underway to test this.

BC is traditionally considered an immunologically suppressive tumor, with the majority showing a lack of lymphocytic infiltration and consequently, modest response rates to immunotherapeutic agents such as anti-programmed cell death protein-1/PD-L1.³⁶ The recruitment of myeloid cells is believed to play a key role in the establishment of this suppressive microenvironment and over time, they can constitute up to 50% of the tumors' mass.^{47 48} In both the syngeneic models studied, we show that the GrB-Fc-KS49 immunotoxin increases the M1 density within the tumor while reducing immunosuppressive M2 macrophages. This response was validated by transcriptomic analysis which showed that the immunotoxin increased the presence of inflammatory cells within the tumor. It is noteworthy that marked changes in the tumor immune microenvironment are observed at doses that are significantly lower than a toxic or fully efficacious dose for other immunotoxins,^{20 22} suggesting that combination therapy with ICIs may further improve efficacy with minimal toxicity. Importantly, the gene profiles obtained post-treatment with the immunotoxin match other studies which show higher immune cell infiltration has the ability to mediate an antitumor immune response. Post-GrB-Fc-KS49 treatment, markers associated with activated CD8+T cells (CD8a, CD8b1, CXCL13, CXCR6),^{49 50} plasma and naïve B cells (CD22),⁵¹ and NK cells⁵² were all upregulated within the tumor. While it is not known if this is due to the activity of the immunotoxin (eg, through the release of GrB), it is unlikely to be due to the induction of antibody-dependent cell cytotoxicity as the KS49 domain at the C-terminus of the Fc domain would block activation of this mechanism of action.²⁰ Additional experiments using flow cytometry and/or single-cell sequencing will

be helpful going forward to define the functionality and density of these populations.

There are several possibilities that may explain how the GrB-Fc-KS49 treatment induced an immune response. The first possibility is that the downregulation of EMP2 alters immune recruitment into the tumor. This is in line with the idea that EMP2 functions as an oncoprotein, changing the composition of the TME.⁵³ The second possibility is that treatment with a GrB immunotoxin elicits an immune response. Traditional views on the function of GrB have been limited to its intracellular proapoptotic role. However, this concept has been challenged as its levels are known to increase within the extracellular matrix in chronic inflammatory responses and alter various extracellular matrix compositions of cytokines, angiogenic factors, and clotting components.^{54 55} With regard to cytokines, for example, studies have shown that GrB can process and activate IL-1 and IL-18 family members, consequently inducing a potent proinflammatory response.^{55 56} Further studies will be needed to test these hypotheses to understand under which conditions GrB functions as a proinflammatory or anti-inflammatory agent within tumors.

Syngeneic mouse models like EMT6 are considered excellent preclinical immune-oncology models. Given the lack of targeted therapies against TNBC, it is notable that the reduction in EMP2 levels during the efficacy study was not significant despite multiple treatments with GrB-Fc-KS49. This suggests neither EMP2 targeting nor GrB delivery impacts EMP2 surface antigen levels. GrB-Fc-KS49 treatment may be worth exploring in chemotherapy-resistant mouse models to understand its potential in treating patients who have developed drug resistance as treatment progresses. Understanding the impact of acquired resistance on EMP2 levels in patient tumors will be crucial in stratifying patients who would benefit from this approach.

While the focus of this study was targeting EMP2 in TNBC, many studies have detailed that the target antigen is also overexpressed in malignancies other than BC including the cell membrane of tumors derived from the ovary, uterus and central nervous system.^{13 15 29 57} Thus, the GrB-Fc-KS49 immunotoxin may be an important addition for treating such malignancies and is a promising therapeutic for further evaluation in various cancers.

Author affiliations

¹Experimental Therapeutics, University of Texas MD Anderson Cancer Center Division of Cancer Medicine, Houston, Texas, USA

²Department of Pathology and Laboratory Medicine, University of California Los Angeles, Los Angeles, California, USA

³Widjaja Inflammatory Bowel Disease Institute, Cedars-Sinai Medical Center, Los Angeles, California, USA

⁴Department of Surgery, University of California Los Angeles, Los Angeles, California, USA

⁵Jonsson Comprehensive Cancer Center, University of California Los Angeles, Los Angeles, California, USA

Present affiliations The present affiliation of Khalid A Mohamedali is: Department of Translational Medical Sciences, Texas A&M University Health Science Center Institute of Biosciences and Technology, Houston, Texas, USA.

X David Casero @DC_Genomics

Acknowledgements The Research Animal Support Facility was supported in part by the University of Texas MD Anderson Cancer Center and P30CA016672 (KAM).

Contributors KAM, DC, MGR, and MW conceived and planned the experiments. BA, C-HL, AC, NK, LL, AMC, LHC, SK, AAdC, and SD contributed to sample preparation and carried out the experiments. KAM took the lead in writing the manuscript. All authors provided critical feedback and helped shape the research, analysis, and manuscript. Final approval of manuscript: All authors. Accountable for all aspects of the work: All authors. Guarantor: MW.

Funding This research was generously supported by the NIH/National Center for Advancing Translational Sciences (NCATS) UL1TR000124, the Iris Cantor-UCLA Women's Health Center/CTSI award (MW), and NCI R21 CA163971 (MW and KAM). Research conducted, in part, by the Clayton Foundation for Research (KAM, LHC, and MGR).

Competing interests MW is an inventor on the University of California patents related to the anti-epithelial membrane protein-2 scFv sequence presented in this work. No other authors have potential conflicts of interest.

Patient consent for publication Not applicable.

Ethics approval Not applicable.

Provenance and peer review Not commissioned; externally peer reviewed.

Data availability statement Data are available upon reasonable request. All data relevant to the study are included in the article or uploaded as supplementary information.

Supplemental material This content has been supplied by the author(s). It has not been vetted by BMJ Publishing Group Limited (BMJ) and may not have been peer-reviewed. Any opinions or recommendations discussed are solely those of the author(s) and are not endorsed by BMJ. BMJ disclaims all liability and responsibility arising from any reliance placed on the content. Where the content includes any translated material, BMJ does not warrant the accuracy and reliability of the translations (including but not limited to local regulations, clinical guidelines, terminology, drug names and drug dosages), and is not responsible for any error and/or omissions arising from translation and adaptation or otherwise.

Open access This is an open access article distributed in accordance with the Creative Commons Attribution Non Commercial (CC BY-NC 4.0) license, which permits others to distribute, remix, adapt, build upon this work non-commercially, and license their derivative works on different terms, provided the original work is properly cited, appropriate credit is given, any changes made indicated, and the use is non-commercial. See <http://creativecommons.org/licenses/by-nc/4.0/>.

ORCID iDs

Khalid A Mohamedali <http://orcid.org/0000-0002-8249-5304>

Anubhav Chandra <http://orcid.org/0009-0001-3999-8811>

Ana Alvarez de Cienfuegos <http://orcid.org/0000-0002-6427-5447>

David Casero <http://orcid.org/0000-0002-7347-3330>

Madhuri Wadehra <http://orcid.org/0000-0001-8514-2021>

REFERENCES

- Königsberg R, Pfeiler G, Kurzawa R, *et al.* Prognostic assessment and adjuvant treatment strategies within early-stage, sporadic triple negative breast cancer patients. *Cancer Invest* 2011;29:180–6.
- Steward L, Conant L, Gao F, *et al.* Predictive Factors and Patterns of Recurrence in Patients with Triple Negative Breast Cancer. *Ann Surg Oncol* 2014;21:2165–71.
- Fournier MV, Goodwin EC, Chen J, *et al.* A Predictor of Pathological Complete Response to Neoadjuvant Chemotherapy Stratifies Triple Negative Breast Cancer Patients with High Risk of Recurrence. *Sci Rep* 2019;9:14863.
- Reck M, Rodríguez-Abreu D, Robinson AG, *et al.* Pembrolizumab versus Chemotherapy for PD-L1-Positive Non-Small-Cell Lung Cancer. *N Engl J Med* 2016;375:1823–33.
- Balar AV, Galsky MD, Rosenberg JE, *et al.* Atezolizumab as first-line treatment in cisplatin-ineligible patients with locally advanced and metastatic urothelial carcinoma: a single-arm, multicentre, phase 2 trial. *Lancet* 2017;389:67–76.
- Robert C, Long GV, Brady B, *et al.* Nivolumab in previously untreated melanoma without BRAF mutation. *N Engl J Med* 2015;372:320–30.
- Wimberly H, Brown JR, Schalper K, *et al.* PD-L1 Expression Correlates with Tumor-Infiltrating Lymphocytes and Response to Neoadjuvant Chemotherapy in Breast Cancer. *Cancer Immunol Res* 2015;3:326–32.
- García-Tejido P, Cabal ML, Fernández IP, *et al.* Tumor-Infiltrating Lymphocytes in Triple Negative Breast Cancer: The Future of Immune Targeting. *Clin Med Insights Oncol* 2016;10:31–9.
- Winer EP, Lipatov O, Im S-A, *et al.* Pembrolizumab versus investigator-choice chemotherapy for metastatic triple-negative breast cancer (KEYNOTE-119): a randomised, open-label, phase 3 trial. *Lancet Oncol* 2021;22:499–511.
- Spring LM, Fell G, Arfe A, *et al.* Pathologic Complete Response after Neoadjuvant Chemotherapy and Impact on Breast Cancer Recurrence and Survival: A Comprehensive Meta-analysis. *Clin Cancer Res* 2020;26:2838–48.
- Wang B, Han Y, Zhang Y, *et al.* Overcoming acquired resistance to cancer immune checkpoint therapy: potential strategies based on molecular mechanisms. *Cell Biosci* 2023;13:120.
- Fu M, Maresh EL, Helguera GF, *et al.* Rationale and preclinical efficacy of a novel anti-EMP2 antibody for the treatment of invasive breast cancer. *Mol Cancer Ther* 2014;13:902–15.
- Fu M, Maresh EL, Soslow RA, *et al.* Epithelial membrane protein-2 is a novel therapeutic target in ovarian cancer. *Clin Cancer Res* 2010;16:3954–63.
- Habeeb O, Goodglick L, Soslow RA, *et al.* Epithelial membrane protein-2 expression is an early predictor of endometrial cancer development. *Cancer* 2010;116:4718–26.
- Wadehra M, Natarajan S, Seligson DB, *et al.* Expression of epithelial membrane protein-2 is associated with endometrial adenocarcinoma of unfavorable outcome. *Cancer* 2006;107:90–8.
- Fu M, Brewer S, Olafsen T, *et al.* Positron emission tomography imaging of endometrial cancer using engineered anti-EMP2 antibody fragments. *Mol Imaging Biol* 2013;15:68–78.
- Gray JE, Heist RS, Starodub AN, *et al.* Therapy of Small Cell Lung Cancer (SCLC) with a Topoisomerase-I-inhibiting Antibody-Drug Conjugate (ADC) Targeting Trop-2, Sacituzumab Govitecan. *Clin Cancer Res* 2017;23:5711–9.
- Nguyen TD, Bordeau BM, Balthasar JP. Mechanisms of ADC Toxicity and Strategies to Increase ADC Tolerability. *Cancers (Basel)* 2023;15:713.
- Tsuchikama K, Anami Y, Ha SYY, *et al.* Exploring the next generation of antibody-drug conjugates. *Nat Rev Clin Oncol* 2024;21:203–23.
- Alvarez de Cienfuegos A, Cheung LH, Mohamedali KA, *et al.* Therapeutic efficacy and safety of a human fusion construct targeting the TWEAK receptor Fn14 and containing a modified granzyme B. *J Immunother Cancer* 2020;8:e001138.
- Cao Y, Mohamedali KA, Marks JW, *et al.* Construction and Characterization of Novel, Completely Human Serine Protease Therapeutics Targeting Her2/neu. *Mol Cancer Ther* 2013;12:979–91.
- Cheung LH, Zhao Y, Alvarez-Cienfuegos A, *et al.* Development of a human immuno-oncology therapeutic agent targeting HER2: targeted delivery of granzyme B. *J Exp Clin Cancer Res* 2019;38:332.
- Mohamedali KA, Cao Y, Cheung LH, *et al.* The functionalized human serine protease granzyme B/VEGF₁₂₁ targets tumor vasculature and ablates tumor growth. *Mol Cancer Ther* 2013;12:2055–66.
- Zhou H, Mohamedali KA, Gonzalez-Angulo AM, *et al.* Development of human serine protease-based therapeutics targeting Fn14 and identification of Fn14 as a new target overexpressed in TNBC. *Mol Cancer Ther* 2014;13:2688–705.
- Voskoboinik I, Whisstock JC, Trapani JA. Perforin and granzymes: function, dysfunction and human pathology. *Nat Rev Immunol* 2015;15:388–400.
- Rosenblum MG, Barth S. Development of novel, highly cytotoxic fusion constructs containing granzyme B: unique mechanisms and functions. *Curr Pharm Des* 2009;15:2676–92.
- Chowdhury D, Lieberman J. Death by a thousand cuts: granzyme pathways of programmed cell death. *Annu Rev Immunol* 2008;26:389:389–420.
- Hlongwane P, Mungra N, Madheswaran S, *et al.* Human Granzyme B Based Targeted Cytolytic Fusion Proteins. *Biomedicines* 2018;6:72.
- Kiyohara MH, Dillard C, Tsui J, *et al.* EMP2 is a novel therapeutic target for endometrial cancer stem cells. *Oncogene* 2017;36:5793–807.
- Hay LZ, Slansky JE. Granzymes: The Molecular Executors of Immune-Mediated Cytotoxicity. *Int J Mol Sci* 2022;23:1833.
- Dillard C, Kiyohara M, Mah V, *et al.* EMP2 Is a Novel Regulator of Stemness in Breast Cancer Cells. *Mol Cancer Ther* 2020;19:1682–95.

- 32 Chan AM, Olafsen T, Tsui J, *et al.* 89Zr-ImmunoPET for the Specific Detection of EMP2-Positive Tumors. *Mol Cancer Ther* 2024;23:890–903.
- 33 Halling Linder C, Englund UH, Narisawa S, *et al.* Isozyme profile and tissue-origin of alkaline phosphatases in mouse serum. *Bone* 2013;53:399–408.
- 34 Serfilippi LM, Pallman DRS, Russell B. Serum clinical chemistry and hematology reference values in outbred stocks of albino mice from three commonly used vendors and two inbred strains of albino mice. *Contemp Top Lab Anim Sci* 2003;42:46–52.
- 35 Majtnerová P, Roušar T. An overview of apoptosis assays detecting DNA fragmentation. *Mol Biol Rep* 2018;45:1469–78.
- 36 Gatti-Mays ME, Balko JM, Gameiro SR, *et al.* If we build it they will come: targeting the immune response to breast cancer. *NPJ Breast Cancer* 2019;5:37.
- 37 Huang X, Cao J, Zu X. Tumor-associated macrophages: An important player in breast cancer progression. *Thorac Cancer* 2022;13:269–76.
- 38 Larionova I, Tuguzbaeva G, Ponomaryova A, *et al.* Tumor-Associated Macrophages in Human Breast, Colorectal, Lung, Ovarian and Prostate Cancers. *Front Oncol* 2020;10:566511.
- 39 Wyckoff JB, Wang Y, Lin EY, *et al.* Direct visualization of macrophage-assisted tumor cell intravasation in mammary tumors. *Cancer Res* 2007;67:2649–56.
- 40 Williams CB, Yeh ES, Soloff AC. Tumor-associated macrophages: unwitting accomplices in breast cancer malignancy. *NPJ Breast Cancer* 2016;2:15025:15025.
- 41 Aran D, Hu Z, Butte AJ. xCell: digitally portraying the tissue cellular heterogeneity landscape. *Genome Biol* 2017;18:220.
- 42 Golej Z, Mahmoodzadeh Hosseini H, Sedighian H, *et al.* Breast cancer targeted/ therapeutic with double and triple fusion Immunotoxins. *J Steroid Biochem Mol Biol* 2020;200:105651.
- 43 Shimazaki K, Lepin EJ, Wei B, *et al.* Diabodies targeting epithelial membrane protein 2 reduce tumorigenicity of human endometrial cancer cell lines. *Clin Cancer Res* 2008;14:7367–77.
- 44 Shimazaki K, Wadehra M, Forbes A, *et al.* Epithelial membrane protein 2 modulates infectivity of Chlamydia muridarum (MoPn). *Microbes Infect* 2007;9:1003–10.
- 45 Dahlin K, Mager EM, Allen L, *et al.* Identification of genes differentially expressed in rat alveolar type I cells. *Am J Respir Cell Mol Biol* 2004;31:309–16.
- 46 Lin W-C, Gowdy KM, Madenspacher JH, *et al.* Epithelial membrane protein 2 governs transepithelial migration of neutrophils into the airspace. *J Clin Invest* 2020;130:127144:157–70.
- 47 Ugel S, De Sanctis F, Mandruzzato S, *et al.* Tumor-induced myeloid deviation: when myeloid-derived suppressor cells meet tumor-associated macrophages. *J Clin Invest* 2015;125:80006:3365–76.
- 48 Racioppi L, Nelson ER, Huang W, *et al.* CaMKK2 in myeloid cells is a key regulator of the immune-suppressive microenvironment in breast cancer. *Nat Commun* 2019;10:2450.
- 49 Dai YW, Wang WM, Zhou X. Development of a CD8⁺ T cell-based molecular classification for predicting prognosis and heterogeneity in triple-negative breast cancer by integrated analysis of single-cell and bulk RNA-sequencing. *Heliyon* 2023;9:e19798.
- 50 Dong H, Xie C, Yao Z, *et al.* PTPRO-related CD8⁺ T-cell signatures predict prognosis and immunotherapy response in patients with breast cancer. *Front Immunol* 2022;13:947841.
- 51 Lv W, He X, Wang Y, *et al.* A novel immune score model predicting the prognosis and immunotherapy response of breast cancer. *Sci Rep* 2023;13:6403.
- 52 Liu Z, Ding M, Qiu P, *et al.* Natural killer cell-related prognostic risk model predicts prognosis and treatment outcomes in triple-negative breast cancer. *Front Immunol* 2023;14:14.
- 53 Gordon LK, Kiyohara M, Fu M, *et al.* EMP2 regulates angiogenesis in endometrial cancer cells through induction of VEGF. *Oncogene* 2013;32:5369–76.
- 54 Boivin WA, Cooper DM, Hiebert PR, *et al.* Intracellular versus extracellular granzyme B in immunity and disease: challenging the dogma. *Lab Invest* 2009;89:1195–220.
- 55 Velotti F, Barchetta I, Cimini FA, *et al.* Granzyme B in Inflammatory Diseases: Apoptosis, Inflammation, Extracellular Matrix Remodeling, Epithelial-to-Mesenchymal Transition and Fibrosis. *Front Immunol* 2020;11:587581.
- 56 Wensink AC, Hack CE, Bovenschen N. Granzymes regulate proinflammatory cytokine responses. *J Immunol* 2015;194:491–7.
- 57 Qin Y, Fu M, Takahashi M, *et al.* Epithelial membrane protein-2 (EMP2) activates Src protein and is a novel therapeutic target for glioblastoma. *J Biol Chem* 2014;289:13974–85.